



## Microstructural Features of Mn<sup>2+</sup> Doped SnO<sub>2</sub> Thin Films

M.C. Rao<sup>1\*</sup>, K. Ravindranadh<sup>1</sup>, A. Kasturi<sup>2</sup>, N. Krishna Mohan<sup>3</sup>,  
M. David Raju<sup>4</sup>, G. Raju<sup>5</sup> and C. Naresh Kumar Reddy<sup>6</sup>

<sup>1</sup>Department of Physics, Andhra Loyola College, Vijayawada - 520 008, India

<sup>2</sup>Department of Physics, Maris Stella College, Vijayawada - 520 008, India

<sup>3</sup>Department of Physics, A. N. R. College, Gudivada-521301, India

<sup>4</sup>PG Department of Chemistry, P.B. Siddhartha College of Arts & Science,  
Vijayawada - 520010, India

<sup>5</sup>Department of Zoology, Osmania University, Hyderabad-500007, India

<sup>6</sup>Department of Physics, Little Flower Degree College, Hyderabad-500036, India

**Abstract:** Tin Oxide (SnO<sub>2</sub>) thin film is one of the important transparent conducting oxides (TCO's) and applied in various fields such as in solar cells, optoelectronic devices, heat mirror, gas sensors, etc due to its electrical and optical transparency in visible light spectrum. Mn<sup>2+</sup> doped tin oxide thin films were prepared by chemical spray pyrolysis synthesis and characterized by different spectroscopic techniques. Powder XRD data revealed that the crystal structure belongs to tetragonal rutile phase and its lattice cell parameters, average crystallite size were evaluated. The morphologies of prepared sample were analyzed by using SEM and TEM studies. Functional groups of the prepared sample were observed in the FT-IR spectrum.

**Keywords:** SnO<sub>2</sub>, Thin films, Spray pyrolysis, Powder XRD, Transmission electron microscope and FT-IR.

### Introduction:

Science and technology of the semiconductor gas sensor was growing rapidly. Device semiconductors gas sensor are generally known as a metal oxide gas sensor because it is made of metal oxides such as TiO<sub>2</sub>, ZnO, CeO<sub>2</sub> and SnO<sub>2</sub> [1]. Semiconductors are used as gas sensors based on the principle of the variability of electrical conductivity of metal oxides when exposed to these gases [2]. These properties can be utilized to detect NO<sub>x</sub>, H<sub>2</sub>, volatile organic compounds (VOCs), SO<sub>x</sub>, CO<sub>2</sub> and O<sub>2</sub>, etc [3]. Metal oxide semiconductor sensor technology is based on the change in resistance of a sensitive metal oxide layer which is induced by the interaction between a surface and ambient gases. Semiconductor oxide thin films are materials with numerous applications in electronic and optoelectronic devices as well as some other applications such as protective coatings, heat mirrors and catalysis [4].

SnO<sub>2</sub> thin films reported in the literature, however, have been obtained mainly by RF magnetron sputtering [5], metal organic chemical vapor deposition [6], vacuum evaporation [7], pulsed laser deposition [8], pulsed electron beam deposition [9], spray pyrolysis [10], sol-gel [11], chemical vapor deposition [12] and successive ionic layer adsorption and reaction [13]. Among these techniques, spray pyrolysis has proved to be simple, reproducible and inexpensive, as well as suitable for large area applications. Besides the simple experimental arrangement, high growth rate and mass production capability for large area coatings make them useful for industrial as well as solar cell applications. In addition, spray pyrolysis opens up the possibility to control the film morphology and particle size in the nm range. As demonstrated [14], spray pyrolysis is a versatile technique for deposition of metal oxides. In the present work, Mn<sup>2+</sup> doped (0.01 mol %) SnO<sub>2</sub> thin

films were prepared by using chemical spray pyrolysis method. The prepared thin films were characterized by powder XRD, SEM with EDS, TEM and FT-IR studies to collect the information about the structural properties of the prepared sample.

### Experimental:

All the chemicals used in the work were of analytical grade.  $Mn^{2+}$  doped  $SnO_2$  thin films were prepared by chemical spray pyrolysis. Spray solution was prepared by mixing 0.1 M aqueous solutions of  $SnO_2$  and  $MnO$  (0.01 mol %) using a magnetic stirrer. The automated spray solution was then transferred to the hot substrate kept at the normalized deposition temperature of 673 K using filtered air as carrier gas at a flow rate normalized to approximately (1.8) ml/min. To prevent the substrate from excessively cooling, the prepared solution was sprayed on the substrate for 10 s with 15 s intervals. The films deposited onto micro-glass slides were first cleaned with detergent water and then dipped in acetone. Powder X-ray diffraction patterns of the prepared samples are recorded on PANalytical Xpert Pro diffractometer with  $CuK\alpha$  radiation. Scanning electron microscope (SEM) and energy dispersive spectrum (EDS) images are taken on ZEISS EVO 18. Transmission electron microscope (TEM) images are recorded on HITACHI H-7600 and CCD CAMERA system AMTV-600 by dispersing samples in ethanol. Bruker FT-IR spectrophotometer is used for recording FT-IR spectrum of the prepared samples in the region  $400-4000\text{ cm}^{-1}$ .

### Results and discussion:

$Mn^{2+}$  doped tin oxide thin films were prepared by chemical spray pyrolysis synthesis and subsequently characterized by Powder XRD, SEM, TEM and FTIR studies.

#### Powder X-ray diffraction studies:

The XRD pattern of  $Mn^{2+}$  doped  $SnO_2$  optimized samples is in good agreement with the reference pattern of tin oxide with standard diffraction data of JCPDS file No. 41-1445. The diffraction data is indexed to tetragonal rutile phase of tin oxide which belongs to the space group  $P4_2/mnm$  and the corresponding lattice cell parameters are evaluated as  $a = b = 0.475\text{ nm}$  and  $c = 0.319\text{ nm}$ . The analysis of X-ray diffraction pattern revealed that the prepared tin oxides films are pure crystalline in nature. It is perceptible from the XRD pattern of  $Mn^{2+}$  doped tin oxide films grow along the preferred orientation of (110). The presence of other orientations such as (101), (200) and (211) has also been detected with considerable intensities. The average crystallite size of the prepared sample is calculated by using Debye-Scherrer's formula,

$$D = (k\lambda/\beta\cos\theta)$$

where  $k$  is a constant (about 0.9),  $\lambda$  is wavelength of X-ray radiation ( $1.5405\text{ \AA}$ ),  $\beta$  is full width at half maximum (FWHM) intensity of the diffraction line and  $\theta$  is diffraction angle. Based on the value of FWHM, the average crystallite size is estimated to be 22 nm, which is in the order of nano-size.

#### Morphological studies:

The morphology and chemical composition of as synthesized thin film was investigated by SEM and EDS analysis. Fig. 1 shows the SEM micrographs of  $Mn^{2+}$  doped  $SnO_2$  thin films taken with different magnifications. It can be clearly observed from low resolution SEM images that, the prepared sample show many agglomerates with an irregular morphology. SEM images reveal that the sample consists of irregular shaped sphere like structures. The incorporation of manganese into the host material was confirmed by EDS measurements. The observed EDS pattern was shown in Fig. 2. The pattern showed the elemental compositions of Sn, O and Mn. From this it was confirmed that the prepared samples contains doped manganese species. TEM measurements were performed to confirm the nano-crystalline nature of the samples and to study the morphology of the particles. The TEM images of  $Mn^{2+}$  doped  $SnO_2$  thin films are depicted in Fig. 3. The particles are more or less uniformed in size and of irregular shape.

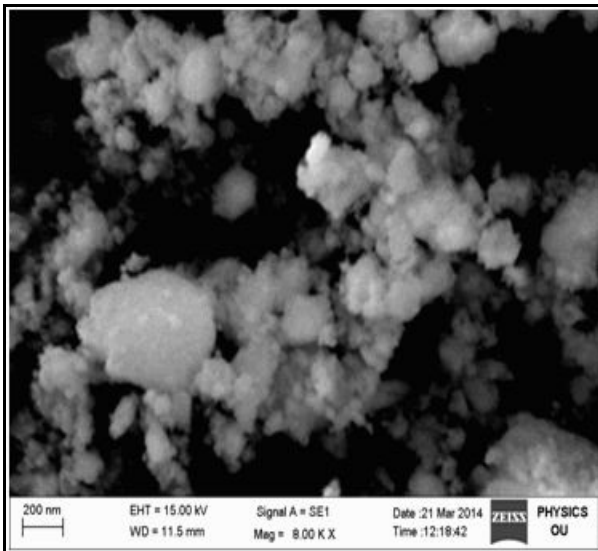


Fig. 1 SEM image of Mn<sup>2+</sup> doped SnO<sub>2</sub> thin films

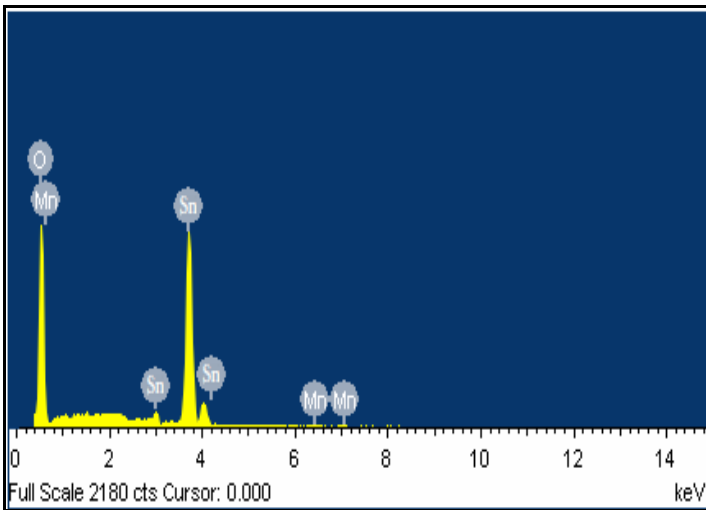


Fig. 2 EDS spectrum of Mn<sup>2+</sup> doped SnO<sub>2</sub> thin films

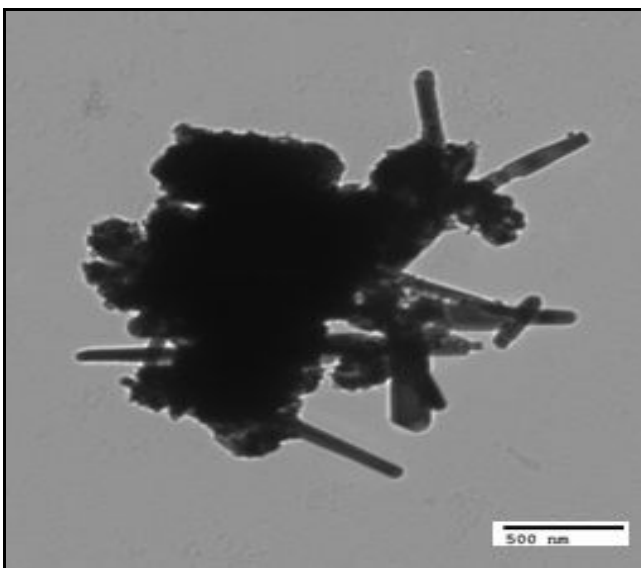


Fig. 3 TEM image of Mn<sup>2+</sup> doped SnO<sub>2</sub> thin films

FT-IR Studies:

FT-IR spectrometry was used for the determination of existing surface species. The FT-IR spectrum of  $\text{Mn}^{2+}$  doped  $\text{SnO}_2$  thin films was illustrated in Fig. 4. The bands at the low wave numbers ( $500\text{-}1000\text{ cm}^{-1}$ ) could be attributed to  $\text{SnO}_2$ . The peaks at  $675$ ,  $784$  and  $966\text{ cm}^{-1}$  were assigned to O–Sn–O, Sn–O–Sn stretching vibrations and lattice vibrations, while the peaks at  $567$  and  $865\text{ cm}^{-1}$  were due to Sn–OH bonds of the  $\text{SnO}_2$  crystalline phase [15]. The bands observed in the region  $2500\text{-}1640\text{ cm}^{-1}$  are due to symmetric and asymmetric vibrations of hydroxyl ions situated at different sites in the lattice.

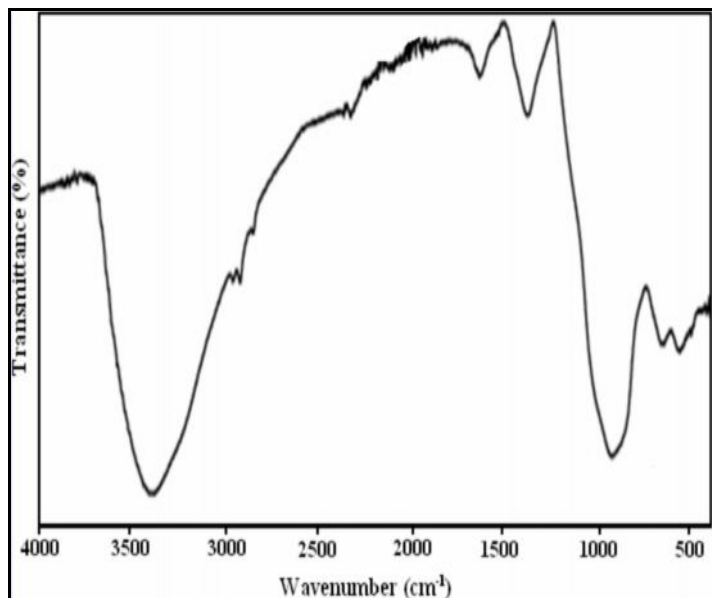


Fig. 4 FT-IR spectrum of  $\text{Mn}^{2+}$  doped  $\text{SnO}_2$  thin films

### Conclusions:

$\text{Mn}^{2+}$  doped  $\text{SnO}_2$  thin films were prepared successfully by chemical spray pyrolysis method. From the powder X-ray diffraction study, the crystal system is indexed to tetragonal rutile phase and the lattice cell parameters are evaluated. The evaluated average crystallite size of  $\text{Mn}^{2+}$  doped  $\text{SnO}_2$  thin films is 22 nm. SEM micrographs shows irregular shaped sphere like structures and EDS analysis confirms the presence of constituent elements of the prepared material. TEM images clearly show the formation of nano rods. FT-IR spectrum showed the characteristic vibrational modes of host lattice.

### References:

1. Kuang Q., Lao C.S., Li Z., Xie Z., Zheng L. and Wang Z., *J. Phys. Chem. C*, 2008, 112, 30-36.
2. Capone S., Forleo A., Francioso L., Rella R., Siciliano P., Spadavecchia J., Presicce D.S. and Taurino A.M., *J. Electron. Mater.*, 2003, 5, 1335-1442.
3. Zhao J., Huo L., Gao S., Zhao H. and Zhao J., *Sens. Actuators B: Chem.*, 2006, 115, 460-464.
4. Malato S., Fernandez-Ibanez P., Maldonado M.I., Blanco J. and Gernjak W., *Catal. Today*, 2009, 147, 1-59.
5. Minami T. and Vac J., *Sci. Technol. A* 1999, 17, 1765-1770.
6. Liu D., Wang Q., Chang H. and Chen H., *J. Mater. Res.* 1995, 10, 1516-1519.
7. Kaito C. and Saito Y., *J. Cryst. Growth* 1986, 79, 403-409.
8. Lamelas F. and Reid S., *Phys. Rev. B* 1999, 60, 9347-9352.
9. Choudhary R., Ogale S., Shinde S., Kulkarni V., Venkatesan T., Harshavardhan K., Strikovski M. and Hannover B., *Appl. Phys. Lett.*, 2004, 84, 1483-1492.
10. Ayouchi R., Martin F., Barrado J., Martos M., Morales J. and Sánchez L., *J. Power Sources*, 2000, 87, 106-111.
11. Baik N., Sakai G., Miura N. and Yamazoe N., *Sens. Actuators B*, 2000, 63, 74-79.
12. Ghoshtagor R., *J. Electrochem. Soc.* 1978, 125, 110-116.
13. Deshpande N., Vyas J. and Sharma R., *Thin Solid Films*, 2008, 516, 8587-8593.

14. Patil P.S., Mater. Chem. Phys., 1999, 59, 185.
15. Khan A.F., Mehmood M., Aslam M. and Ashraf M., Appl. Surf. Sci. 2010, 256, 2252-2257.

**\*\*\*\*\***